Optics Communications 432 (2019) 97–100

Contents lists available at ScienceDirect

Optics Communications

journal homepage: www.elsevier.com/locate/optcom

Enhancement of Signal Performance in bidirectional RSE-based CVLC system employing NPM modulation scheme

Rui Deng [a,b], Jing He [a,*], Gee-kung Chang [b]

[a] College of Computer Science and Electronic Engineering, Hunan University, Changsha 410082, China
[b] School of Electrical and Computer Engineering, Georgia Institute of Technology, Atlanta, GA, 30308, USA

ARTICLE INFO

Keywords:
Visible light communication (VLC)
Rolling shutter effect (RSE)
Modulation
Digital signal processing (DSP)

ABSTRACT

Camera-based visible light communication (CVLC) exploiting rolling shutter effect (RSE) is a cost-effective technique that ensures secure data transmission. In this paper, a bidirectional CVLC system is experimentally demonstrated using smartphone/laptop as downlink/uplink transceiver in an experimental prototype testbed. Meanwhile, a Nyquist pre-distorted Manchester (NPM) modulation scheme is proposed and validated in the experimental testbed system. The proposed scheme is based on low-complexity transmitter-side digital signal processing (DSP) techniques, Nyquist shaping and linear pre-distortion, which can be employed for mitigation of the impact of extinction ratio (ER) fluctuation and exposure overlapping in the RSE-based CVLC system. The experimental results show that by using the proposed NPM modulation, the uplink and the downlink can both achieve about 4.8 Kb/s transmission with bit error rate (BER) of below than 3.8e−3. It verifies the effectiveness of the proposed NPM scheme and the corresponding transmitter-side DSP techniques.

1. Introduction

By controlling the on–off state of light emitting diode (LED), data can be modulated onto visible light. By exploiting the rolling shutter effect (RSE) of camera image sensor, the data can be demodulated from the received lightwave signal correspondingly. Based on this principle, a camera-based visible light communication (CVLC) system can be realized by using commercial LEDs as the transmitter and smartphones as the receiver. Compared with legacy photodetector (PD)-based VLC system [1], CVLC system is more cost-effective as CMOS imaging IC is an essential built-in component in smart mobile phones. Moreover, compared with traditional screen-based CVLC system [2], RSE-based CVLC system using LED does not need to consider geometrical distortion in the receiver and it would be tolerant to motion [3]. Hence, RSE-based CVLC technology has attracted more attention of researchers recently [4–7]. Meanwhile, due to its inherent advantages such as immunity to electromagnetic interference (EMI), physical link security, ease of installation and low cost, RSE-based CVLC is capable to meet the demand of many system applications, including indoor positioning [8], communication encryption [9] and visible light identification (VLID) [10].

As we know, near-field communication (NFC) brings great convenience to enrich people's life because it enables applications like electronic wallet for low-value payments and access control system. Common NFC is based on radio frequency identification (RFID) [11]. However, RF system would generate EMI and is not suitable for EMI-sensitive application scenario [12]. At present, CVLC-based VLID would be an alternative and effective solution for NFC [13]. Compared with RFID NFC, VLID NFC can be deployed in EMI-sensitive environment. Moreover, the direction and distance of the CVLC link between the LED and camera can be easily controlled, preserving communication privacy and security. In addition, in VLID NFC applications, the smartphone apps can be used in the place of conventional contactless magnetic cards and meanwhile it does not require laborious integration of NFC chips into the smartphone or other related device. However, the deployment of VLID NFC technology is facing many challenges including extinction ratio (ER) fluctuation, exposure overlapping, and sampling frequency offset (SFO), etc. Fortunately, most of the challenges can be overcome by using advanced digital signal processing (DSP) algorithm [14–16]. For example, based on moving exponent averaging (MEA) [14], the ER fluctuation can be effectively mitigated; based on entropy thresholding [15], logic decision for data recovery can be realized effectively even when serious blooming occurs; based on Sobel filter [16], valid edge detection can be realized in the received data with exposure overlapping. Nevertheless, most of the DSP schemes are on the receiver side and they were proposed by researches of unidirectional CVLC. Due to the DSP function resides in the receiver, it will increase the complexity and the runtime of the receiver; it will incur long communication delays in a bidirectional CVLC system.

In this paper, we experimentally demonstrate a bidirectional RSE-based CVLC system using a simple set-up consisting of a smartphone and a laptop PC. To our knowledge, we demonstrate for the first

* Corresponding author.
E-mail address: jhe@hnu.edu.cn (J. He).

https://doi.org/10.1016/j.optcom.2018.09.067
Received 20 August 2018; Received in revised form 26 September 2018; Accepted 27 September 2018
Available online 3 October 2018

time, a Nyquist pre-distorted Manchester (NPM) modulation scheme for CVLC. In this scheme, Nyquist shaping and pre-distortion techniques are employed in the transmitter to mitigate the effect of exposure overlapping and ER fluctuation. The performance of the bidirectional CVLC system is evaluated experimentally, and the effectiveness of the proposed NPM scheme has been verified.

2. Experimental setup

Fig. 1 shows the experimental setup of the bidirectional RSE-based CVLC system and the DSP flowchart of the NPM scheme. In the system, the smartphone (Xiaomi Mi 4, which is equipped with a 13 million pixels camera) is used as downlink transceiver and the laptop (Intel i7-6700HQ CPU@2.60 GHz) equipped with a 720P camera is used as uplink transceiver. The process of the uplink can be described as follows. The original electrical signal is generated from the audio output port of the smartphone at first. Through an audio plug connector and audio cable, the signal is injected into an audio electrical amplifier (EA) for amplification. Then, the amplified signal is used to modulate the intensity of the light from the LED. After 5-cm free-space transmission, a white paper is used as light diffuser to diffuse the modulated light from the LED. Subsequently, by photography using the camera of the laptop, the modulated light can be captured into photos and the signal would be recorded in photos due to RSE of the camera. At last, the photos are uploaded to the self-designed application program in laptop for signal demodulation.

It should be noted that, to generate the original electrical signal, another self-designed application program in smartphone is used. In the uplink communication, the function of the application program in smartphone is used to realize the DSPs of the transmitter part for NPM modulation as shown in Fig. 1(b) (TX) to control the audio output. The DSP functions of the transmitter part includes: (1) PRBS generation. A pseudo-random binary sequence (PRBS) including 150 binary digits is pre-stored as the original data and transmitted periodically; (2) Manchester Encoding; (3) Header (HD) insertion. The data sequence [0, 1, 1, 1, 1, 0] is used as a header in the encoded data sequence for the synchronization of the receiver; (4) Pre-distortion; (5) Nyquist shaping. Among them, pre-distortion and Nyquist-shaping are used to mitigate the effect of ER fluctuation and exposure overlapping respectively and thereby enhance the performance of the received signal in the system. In the later part of this paper, (4) pre-distortion and (5) Nyquist shaping function depicted above will be illustrated in detail.

Meanwhile, the function of the application program in laptop is to realize the DSPs of the receiver part for NPM demodulation as shown in Fig. 1(b) (RX) and analyze the transmission performance. The DSPs of the receiver part includes: (1) Read Image. Convert the photo into gray one and read its grayscale value; (2) Column selection. Select a proper column in the matrix of the grayscale data of the photo; (3) Synchronization. The header in the received signal can be used for a timing synchronization and then the valid data in the received signal can be extracted; (4) Logical Decision. A decision process is used to recover the logic data 1 and 0; (5) BER calculator. In a similar way, the process of the downlink is realized by using the laptop as transmitter and using the smartphone as receiver. The difference is that the resolution of the photo captured by the camera of the laptop is 1280×720 in the process of the uplink while the resolution of the photo captured by the camera of the smartphone is 4208×3120 in the process of the downlink.

3. The principle of the proposed transmitter-side DSP schemes

Fig. 2(a)/(b) shows the model of LED ideal and practical illuminance before/after pre-distortion is used. As analyzed in Ref. [14], due to the capacitive characteristics of LED, the emitted light is gradually brighten, which will result in the high ER fluctuation. As shown in Fig. 2(a), if the signal amplitude of the consecutive "1, 1" symbol is same as that of the independent "1" symbol at the transmitter side, it will result in imbalanced received illuminance. In the NPM scheme, to make received illuminance balanced by adjusting the amplitude of different data symbols in transmitter, a simple pre-distortion scheme is proposed as

$$\boldsymbol{P}(i) = \begin{cases} \alpha \cdot \boldsymbol{M}(i), \boldsymbol{M}(i+1) == \boldsymbol{M}(i) \\ \alpha \cdot \boldsymbol{M}(i), \boldsymbol{M}(i-1) == \boldsymbol{M}(i) \\ \boldsymbol{M}(i), others \end{cases} \tag{1}$$

where $\boldsymbol{M}$ sequence is the sequence of the Manchester encoded data, $\boldsymbol{P}$ sequence is the sequence of the data after pre-distorted and α is a constant which should be chosen properly in experiment. It is imagined that after pre-distortion is used, although there is an amplitude fluctuation in the transmitted data sequence, the received illuminance will be balanced, as shown in Fig. 2(b).

Fig. 3(a) shows the phenomenon of impulse broadening induced by exposure overlapping. Exposure overlapping is one of the main factors limiting the transmission performance in RSE-based CVLC system [5] because it is the primary reason of the image blurring [17] in RSE-based CVLC. As shown in Fig. 3(a), it will lead to serious impulse broadening in CVLC system and thereby cause inter-code interference (ICI) during the data transmission. To mitigate overlapping-induced ICI, special Nyquist shaping is applied in the NPM scheme and it can be expressed as

$$\boldsymbol{S} = \boldsymbol{I} * \boldsymbol{N} \tag{2}$$

where S is the data sequence after Nyquist shaping, * represents the convolution operation, N sequence is the truncated Nyquist pulse sequence, and I sequence is the sequence of the pre-distorted data after zero padding which can be expressed as

$$\boldsymbol{I}(i) = \sum_{i=1}^{TL} \sum_{l=1}^{L} \boldsymbol{P}(l) \cdot \delta[i - Tl + round\left(\frac{T}{2}\right)] \tag{3}$$

where $\delta(\cdot)$ represents unit impulse function, $round(\cdot)$ represents rounding function, L is the length of P sequence, and T is an integer constant which decides the number of the padded zeros. Commonly, by using moderate transmitter sampling rate, the transmitted signal will be rectangle shaped in default due to the zero-order hold effect of digital-to-converter (DAC), as shown in Fig. 3(b)(1). In the proposed NPM scheme, by using relatively high sampling rate, the transmitted signal is shaped by Nyquist pulse as shown in Fig. 3(b)(2).

4. Experimental results and discussions

To verify the effectiveness of the proposed DSPs and evaluate the performance of the bidirectional CLVC system, the uplink transceiver and the downlink transceiver work simultaneously and shoot photos continuously in the experiment. By randomly selecting a part of photos for analysis, a serial of experimental results are obtained. Fig. 4(a) shows a fragment of the received signal (the grayscale data of one column of one captured photo) when Nyquist shaping and pre-distortion are not applied in the transmitter. Fig. 4(b) shows a fragment of the received signal when only pre-distortion are used in the transmitter. Fig. 4(c) shows a fragment of the received signal when Nyquist shaping and pre-distortion are both used in the transmitter. Obviously, the ER imbalance has been mitigated by using pre-distortion scheme and the unclear symbol boundary induced by exposure overlapping. It should be mentioned that α is set at 0.7 for pre-distortion in our experiment. When α is much larger than 0.7, the pre-distortion mayn't compensate the imbalance between the received illuminance of consecutive "1, 1" symbol and independent "1" symbol. In addition, when α is much less than 0.7, the received illuminance of consecutive "1, 1" symbol will be lower than the received illuminance of independent "1" symbol. It can also incur an imbalance. Hence, an appropriate value for α is about 0.7 in our experiment.

Fig. 4(d) shows the measured BER performance of the downlink transmission. Fig. 4(e) shows the measured BER performance of the uplink transmission. It is obvious that either in the uplink transmission

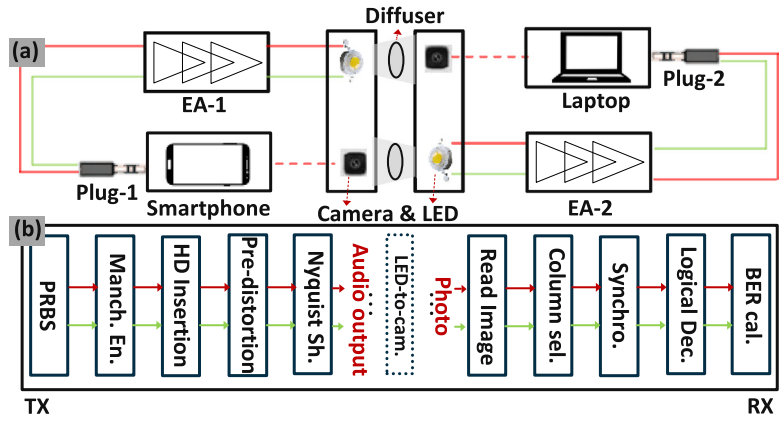

Fig. 1. Experimental setup. EA: electrical amplifier. PRBS: Pseudo-Random Binary Sequence generator. Manch. En. : Manchester Encoder. Nyquist Sh. : Nyquist Shaping. LED-to-cam.: LED-to-camera. Column sel. : Column selection. Synchro. : Synchronization. Logical Dec. : Logical Decision. BER cal. : BER calculator.

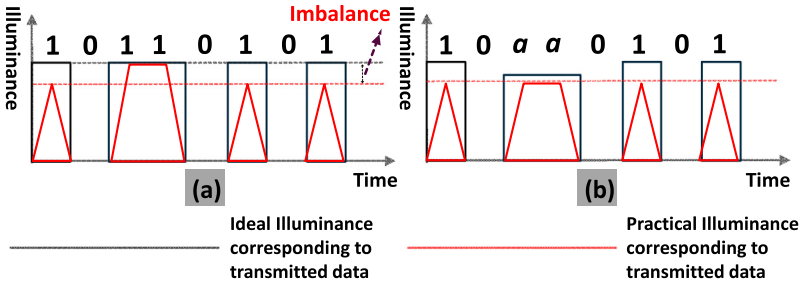

Fig. 2. (a) the model of ideal LED with practical characteristics of illuminance before pre-distortion is used; (b) the model of an ideal LED with practical illuminance after pre-distortion is used.

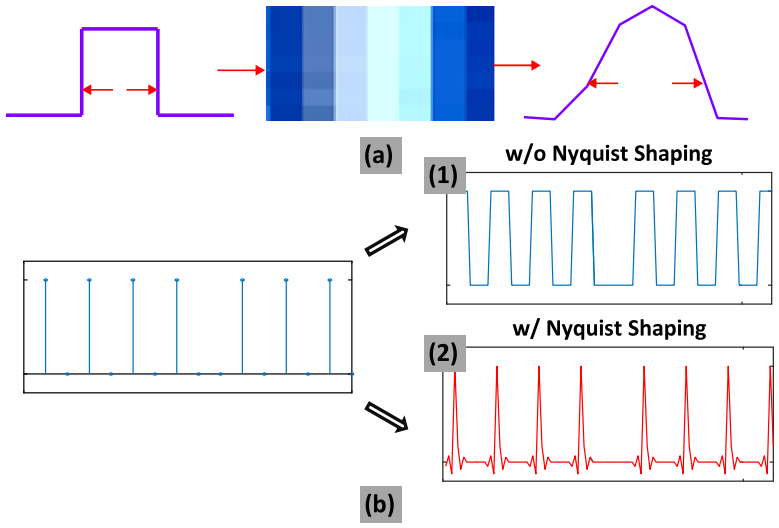

Fig. 3. (a) Impulse broadening phenomenon caused by exposure overlapping. (b) Comparison of the transmitted signal before and after Nyquist shaping is applied.

or the downlink transmission, Nyquist shaping and pre-distortion can both improve the transmission performance effectively. When the illuminance is beyond 500 lux, the uplink/downlink can achieve a BER below than 3.2e−3 ($10^{-2.5}$). In addition, it can be found that, there is an overlapping for blue and pink curves in Fig. 4(d) and (e). In my opinion, this is because that, when the illuminance is too low, dimming induced image blurring becomes the main limitation factor for the transmission performance since dimming can also result in an overlapping effect between adjacent pixels in adjacent rows and columns. However, the effect of image blurring induced by dimming is not considered in our experiment. It can affect the effectiveness of the applied techniques.

Fig. 4(f) shows one sample of the received signal in the uplink. Fig. 4(g) shows one sample of the received signal in the downlink. As we can see from the figures, in the uplink transmission, one bit only occupies about 4 pixels, and in the downlink transmission, one bit only occupies about 6 pixels. Hence, in the uplink, one frame of photo can carry about 180 bits and in the uplink, one frame of photo can carry about 520 bits. In our experiment, after considering the overhead of the synchronization header, the data rate of the uplink would be about 0.16 Kb/s/frame and the data rate of the uplink would be about 0.48 Kb/s/frame.

In addition, an extra experiment is carried out based on continuous photo mode. In the additional experiment, the downlink and the uplink

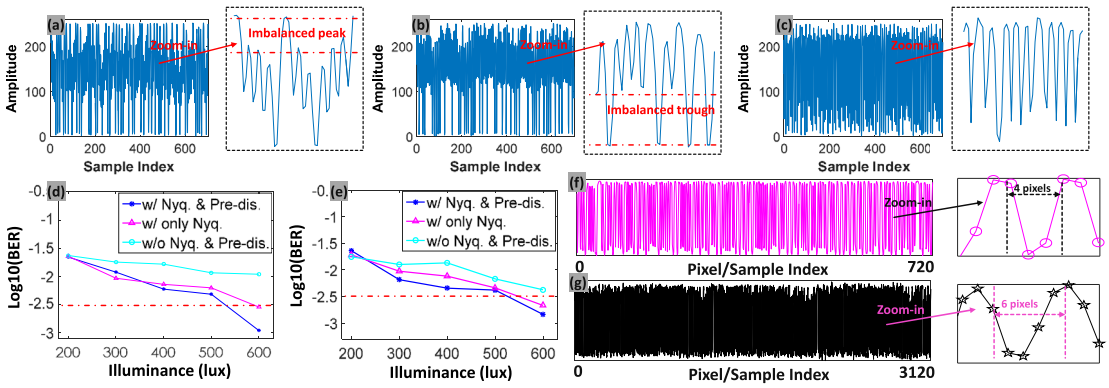

Fig. 4. Experimental results. A fragment of the received signal in the case (a) w/o Nyquist shaping & pre-distortion, (b) w/ only pre-distortion and (c) w/ Nyquist shaping & pre-distortion. (d) Measured BER performance of the downlink transmission. (e) Measured BER performance of the uplink transmission. (f) One sample of the received signal in the uplink. (g) One sample of the received signal in the downlink. (For interpretation of the references to color in this figure legend, the reader is referred to the web version of this article.)

Table 1
The result of the additional experiment.

(Rate, BER)@Downlink	(Rate, BER)@Uplink	(Rate, BER)@Downlink
(4.8 Kb/s, 1.56e−3)	(4.8 Kb/s, 2.38e−3)	(4.8 Kb/s, 1.56e−3)

take photos continuously for several seconds and the obtained photos are uploaded to a personal computer for offline processing to further evaluate the performance of the system. Table 1 shows the result of the additional experiment. Due to that the frame rate of the smartphone camera and the laptop camera can be set at 30 frame/s and 10 frame/s respectively, the uplink and the downlink can both realize an up to 4.8 Kb/s (uplink: 0.16 Kb/s/frame × 30 frame/s; downlink: 0.48 Kb/s/frame × 10 frame/s) transmission with a BER of below than 3.8e−3, the hard decision forward error correction (HD-FEC) limit, as shown in Table 1.

5. Conclusion

In this paper, we demonstrated a bidirectional RSE-based CVLC system employing a novel NPM modulation scheme. The DSPs of the NPM scheme are introduced in detail. Moreover, key system operation requirements of the system are also introduced. The performance of the system has been evaluated in an experimental testbed. Meanwhile, the effectiveness of the NPM scheme and its corresponding transmitter-side DSP techniques has been verified. In the system, the uplink transmission and the downlink transmission can both achieve a data rate of about 4.8 Kb/s. Our experimental results has proved the feasibility of the bidirectional CVLC exploiting RSE. It would be an effective technology for low-speed near-field applications such as payment transactions in supermarket or department stores and control access system.

Acknowledgments

This work was supported in part by National Natural Science Foundation of China under Grant 61775054 and Grant 61377079; and in part by Science and Technology Project of Hunan Province, China (2016GK2011); and in part by Hunan Provincial Innovation Foundation, China for Postgraduate (CX2017B100).

References

[1] K. Ying, H. Qian, R.J. Baxley, S. Yao, Joint optimization of precoder and equalizer in MIMO VLC systems, IEEE J. Sel. Areas Commun. 33 (9) (2015) 1949–1958.
[2] R. Boubezari, H. Le Minh, Z. Ghassemlooy, A. Bouridane, Smartphone camera based visible light communication, J. Lightwave Technol. 34 (17) (2016) 4121–4127.
[3] R. Deng, J. He, Y. Hong, J. Shi, L. Chen, 2.38 Kbits/frame WDM transmission over a CVLC system with sampling reconstruction for SFO mitigation, Opt. Express 25 (24) (2017) 30575–30581.
[4] C. Danakis, M. Afgani, G. Povey, I. Underwood, H. Haas, Using a CMOS camera sensor for visible light communication, in: 2012 IEEE Globecom Workshops, 2012, p. 1244.
[5] C.W. Chow, C.Y. Chen, S.H. Chen, Visible light communication using mobile-phone camera with data rate higher than frame rate, Opt. Express 23 (20) (2015) 26080–26085.
[6] J. Shi, J. He, J. He, R. Deng, Y. Wei, F. Long, Y. Cheng, L. Chen, Multilevel modulation scheme using the overlapping of two light sources for visible light communication with mobile phone camera, Opt. Express 25 (14) (2017) 15905–15912.
[7] D.T. Nguyen, Y. Park, Data rate enhancement of optical camera communications by compensating inter-frame gaps, Opt. Commun. 394 (2017) 56–61.
[8] M. Liu, K. Qiu, F. Che, S. Li, B. Hussain, L. Wu, C. Patrick Yue, Towards indoor localization using Visible Light Communication for consumer electronic devices, in: 2014 IEEE/RSJ International Conference on Intelligent Robots and Systems, 2014, p. 143.
[9] Y. Liu, K. Liang, H.Y. Chen, L.Y. Wei, C.W. Hsu, C.W. Chow, C.H. Yeh, Light encryption scheme using light-emitting diode and camera image sensor, IEEE Photo J. 8 (1) (2016) 1–7.
[10] S.J. Song, H. Nam, Visible light identification system for smart door lock application with small area outdoor interface, Curr. Opt. Photon 1 (2) (2017) 90–94.
[11] J.H. Ahn, S.H. Lee, T.J. Lee, Anti-collision protocol for coexistence of RFID and NFC P2P communications, IEEE Commun. Lett. 20 (11) (2016) 2185–2188.
[12] M. Chen, J. He, L. Chen, Real-time optical OFDM long-reach PON system over 100 km SSMF using a directly modulated DFB laser, IEEE/OSA J. Opt. Commun. Networking 6 (1) (2014) 18–25.
[13] J. Niu, F. Gu, R. Zhou, G. Xing, W. Xiang, VINCE: Exploiting visible light sensing for smartphone-based NFC systems, in: IEEE Conference on Computer Communications, INFOCOM, 2015, p. 2722.
[14] Z. Zhang, T. Zhang, J. Zhou, Y. Qiao, A. Yang, Y. Lu, Performance enhancement scheme for mobile-phone based VLC using moving exponent average algorithm, IEEE Photo J. 9 (2) (2017) 1–7.
[15] Kevin Liang, Chi-Wai Chow, Yang Liu, Chien-Hung Yeh, Thresholding schemes for visible light communications with CMOS camera using entropy-based algorithms, Opt. Express 24 (22) (2016) 25641–25646.
[16] C.W. Chow, C.Y. Chen, S.H. Chen, Enhancement of signal performance in LED visible light communications using mobile phone camera, IEEE Photo J. 7 (5) (2015) 1–7.
[17] S. Pergoloni, M. Biagi, S. Colonnese, R. Cusani, G. Scarano, A space-time RLS algorithm for adaptive equalization: The camera communication case, J. Lightwave Technol. 35 (10) (2017) 1811–1820.